Journal of Inclusion Phenomena and Molecular Recognition in Chemistry **18:** 177–192, 1994.

Crystalline Complexes, Coordination Polymers and Aggregation Modes of Tetra(4-pyridyl)porphyrin

HELENA KRUPITSKY, ZAFRA STEIN and ISRAEL GOLDBERG*
School of Chemistry, Sackler Faculty of Exact Sciences, Tel-Aviv University, 69978 Ramat-Aviv, Israel

and

CHARLES E. STROUSE*
Department of Chemistry and Biochemistry, University of California, Los Angeles, CA 90024–1569, U.S.A.

(Received: 23 February 1994; in final form: 17 June 1994)

Abstract. Aggregation patterns of tetra(4-pyridyl)porphyrin and of its zinc(II) complex in seven new solid materials have been investigated by X-ray diffraction. The metalloporphyrin compound forms two types of coordination polymers through ligation of the porphyrin periphery on one molecule to the metal center of an adjacent porphyrin. These include one-dimensional chains with a zigzag conformation, as well as three-dimensional, extensively interlinked, polymeric structures. The non-metallated compound reveals a characteristic layered arrangement and interporphyrin stacking of the type which is commonly observed in the structures of tetraphenylporphyrin derivatives. In the absence of a metal center, the basic functionality of the pyridyl substituents is utilized for effective H-bond directed coordination and co-crystallization with solvent/guest components. The stoichiometry of the porphyrin solvation, and the consequent interporphyrin organization in the solid phase, are quite sensitive to the nature of the coordinating solvent.

Key words: Tetra(4-pyridyl)porphyrin, crystalline complexes of, aggregation modes of, coordination polymers.

Supplementary Data relating to this article are deposited with the British Library as supplementary publication No. SUP 82174 (37 pages).

1. Introduction

Porphyrin and tetraarylporphyrin molecules reveal unique modes of aggregation in solution [1], in thin layers [2], as well as in crystalline solids. Earlier systematic investigations of solids have ellucidated the remarkable versatility of tetraphenyl-metalloporphyrin complexes as formers of crystalline heteromolecular materials [3], as well as the structural systematics of the porphyrin host lattice which is dominated primarily by the molecular shape [4–6]. Additional control of the intermolecular aggregation modes can be obtained by introduction of functional substituents on the porphyrin periphery. Moreover, functionalization of the rigid porphyrin molecular frameworks with polarized aryl groups can be used to develop

* Authors for correspondence.

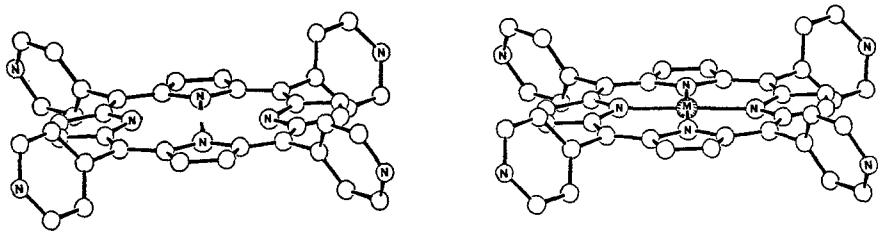

Fig. 1. Illustration of the molecular structures of the TPyP (left) and metallated TPyP (right).

simple chemical models of self-assembly *via* weak intermolecular forces. Successful results of such self-assembling have been achieved in a recent solution study [7]. We have also confirmed the validity of these structure-engineering concepts in the solid phase of the porphyrin materials, and demonstrated that the type of supramolecular assembling in the crystal can be controlled by molecular design [8,9].

In the previous report two families of crystalline aggregates, in which the functionalized tetra(4-X-phenyl)porphyrin molecules (where X=OH or Cl) are linked into pseudo-rigid two-dimensional and three-dimensional polymeric patterns *via* hydrogen-bonding and Cl· · ·Cl interactions, have been described [8]. The resulting solids have a characteristic hollow architecture (different combinations of interporphyrin cavities and canals, the size and shape properties of which are determined by the directional intermolecular interactions), and a strong tendency to absorb guest molecules within the lattice. They thus represent a novel type of microporous materials suitable e.g., for isolation, separation and slow release of molecular moieties. The current study deals with characterizations of intermolecular aggregation modes in structures based on the tetra(4-pyridyl)porphyrin (TPyP) building blocks [10] in various stoichiometric combinations with molecular guest solvents. In these molecules, binding sites on the porphyrin periphery are provided by the pyridyl nitrogens and their lone-pair electrons. Ligation of pyridyl moieties to the metal center of metalloporphyrins, and its utilization in templated synthesis have previously been reported [1]. Formation of oligomers involving pyridine meso-substituted porphyrins, axially coordinated to other metalloporphyrins, has also been confirmed by spectroscopic methods. The authors are aware, however, of only a very small number of detailed crystallographic characterizations of the tetrapyridylporphyrin materials, most probably due to the severe difficulties usually experienced in growing suitable crystals for diffraction experiments. Earlier determinations include the crystal structures of the diacid tetra(4-pyridyl)porphyrin-6-(hydrogen chloride) [11], and of tetra(4-pyridyl)-Zn-porphyrin with pyridine [12]. Crystallographic analyses of the monopyridyltriphenyl-Zn-porphyrin (Zn-MPyTPP) [13], and the tetra(*o*-nicotinamidophenyl)-Fe-porphyrin, which also contains pyridyl rings on the molecular periphery [14], have been published more recently.

We report here on the structures of seven new materials based on tetra(4-pyridyl)porphyrin and on its mononuclear zinc complex (See Figure 1), ellucidating the typical interporphyrin aggregation modes and conditions of their occurrence.

2. Experimental

Tetrapyridylporphyrin (TPyP) and Zn-tetrapyridylporphyrin were purchased from Midcentury Chemicals (Posen, Illinois). The various compounds (see below) were obtained by recrystallization of the porphyrin derivative from a minimum amount of the respective liquid. Common solvents (such as: methanol, glacial acetic acid, ethyl acetate) were used in some cases to control the solubility of the tetrapyridylporphyrin derivative. Suitable crystals for X-ray diffraction were prepared in various ways, including slow cooling, solvent diffusion, and solvent evaporation in open air for long periods of time (several weeks). The crystalline compounds subjected to a detailed structural investigation are:

1. Zn–TPyP [$C_{40}H_{24}N_8Zn$];
2. Zn–TPyP · aniline [$C_{40}H_{24}N_8Zn \cdot C_6H_7N$] 1 : 1;
3. Zn–TPyP · methanol · water [$C_{40}H_{24}N_8Zn \cdot CH_3OH \cdot H_2O$] 1 : 1 : 2;
4. Zn–TPyP · water [$C_{40}H_{24}N_8Zn \cdot H_2O$] 1 : 3;
5. TPyP · guaiacol [$C_{40}H_{26}N_8 \cdot C_7H_8O$] 1 : 2;
6. TPyP · benzyl alcohol [$C_{40}H_{26}N_8 \cdot C_7H_8O$] 1 : 2;
7. TPyP · *o*-chlorophenol [$C_{40}H_{26}N_8 \cdot C_6H_5ClO$] 1 : 5.

The X-ray diffraction experiments were carried out at room temperature on automated CAD4 (compounds **1–2** and **4–7**) and Picker (compound **3**) diffractometers equipped with a graphite monochromator. Intensity data were collected by the $\omega - 2\theta$ scan mode with a constant speed (2.0, 3.0 or 4.0 deg/min, according to the diffraction power of the analyzed crystal), using MoK_α radiation ($\lambda = 0.7107$ Å). Three standard reflections from different zones of the reciprocal space were measured periodically, with no significant variation. No corrections for absorption and secondary extinction effects were applied; attempts to introduce empirical absorption corrections of the data sets did not improve the quality of the results. The crystal data and pertinent details of the experimental conditions are summarized in Table I.

The crystal structures were solved by a combination of direct methods (MULTAN-80, [15] and SHELXS-86, [16]). Their refinements were carried out by either a full-matrix or large-block least-squares, including the positional and thermal parameters of the non-hydrogen atoms. The refinement calculations were based on F for structures **1–3** (SHELX-76, [17]), and on F^2 for structures **4–7** (SHELXL-93, [18]); the hydrogen atoms were introduced in calculated positions, the methyls being treated as rigid groups. In most cases, the refinements converged at reasonably low R-values (Table I), allowing a reliable description of the atomic parameters

TABLE I. Summary of crystal data and experimental parameters

Compound	**1**	**2**	**3**	**4**	**5**	**6**	**7**
FW[a]	682.1	775.2	750.1	736.1	867.0	835.0	1261.5
Space group	$P2_1/c$	$C2/c$	$R\bar{3}$	$R\bar{3}$	$P\bar{1}$	$P\bar{1}$	$P\bar{1}$
Z	4	8	9	9	1	1	1
a, Å	11.187(4)	26.318(4)	33.032(9)	33.145(3)	6.784(1)	6.406(3)	6.325(3)
b, Å	13.825(1)	13.810(2)	33.032	33.145	10.117(1)	10.292(2)	14.153(7)
c, Å	22.172(3)	23.749(5)	9.252(3)	9.374(3)	16.589(2)	17.412(2)	17.543(2)
α, deg	90.0	90.0	90.0	90.0	80.55(2)	74.54(1)	101.02(4)
β, deg	100.52(2)	115.61(2)	90.0	90.0	87.38(1)	83.20(2)	96.62(4)
γ, deg	90.0	90.0	120.0	120.00	77.65(2)	79.29(2)	95.50(4)
V, Å^3	3371.5	7783.6	8742.1	8918.5	1097.1	1084.3	1519.9
D_c, g cm^{-3}	1.34	1.32	1.28	1.23	1.31	1.28	1.38
$F(000)$	1400	3200	3492	3420	454	438	652
μ, cm^{-1}	7.84	6.88	6.92	6.77	0.79	0.75	2.96
2θ limits, deg	50	46	46	50	50	50	46
N(unique)	5065	4897	2221	3362	3386	3123	3285
N(obs)[b]	2184	3296	1354	2582	2488	1988	1657
R_F	0.081	0.060	0.071	0.056	0.055	0.091	0.105
$\lvert\Delta\rho\rvert_{max}$	0.68	0.52	0.68	0.72	0.38	0.48	0.88

[a] Formula weights refer to the compositions defined in the text.

[b] For compounds **1–3** $I > 3\sigma(I)$, for **4–7** $I > 2\sigma(I)$.

and of the intermolecular interaction scheme. Some difficulties experienced in the refinement procedures, similar to those typically observed in related studies of composite porphyrin structures [5,8,19], are detailed below.

Electron density difference maps for compounds **3** and **4** showed significant residual peaks, indicating that, in addition to the pyridyl-bound water, other solvent molecules (apparently, methanol in **3** and water in **4**) are contained in the interporphyrin cavities. These were introduced in the corresponding refinements with partial occupancies. The exact solvent contents of crystals **3** and **4** could not be assessed reliably either by structure-factor refinement, due to the high correlation between the (partial) occupancy and thermal motion parameters, or by elemental analysis. Therefore, the porphyrin-solvent stoichiometric composition of these crystals defined above represents only an approximation.

In structures **1**, **2** and **7**, excessively large thermal motion parameters for the peripheral pyridyl groups (apparently due to loose crystal packing), and a relatively low data-to-parameters ratio, dictated a geometrically constrained refinement of the pyridyl rings. Similar constraints were applied to the aromatic guest/solvent components in **2** and **5–7**. Moreover, in compound **2**, two of the pyridyl rings and the aniline solvent were found to exhibit a twofold orientational disorder. Structural disorder is also characteristic to the benzyl alcohol guest in **6** (modeled in the

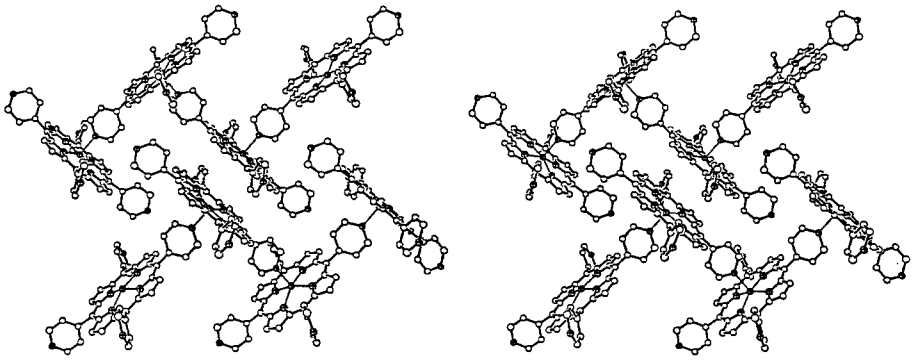

Fig. 2. Stereoview of the coordination polymers of Zn–TPyP in **1** (4-monomer sections are shown), illustrating their zigzag conformation and tight packing in the crystal structure. The zinc and nitrogen atoms are marked by crossed circles. All Zn–N coordinations are denoted by thin solid lines.

refinement as a twofold positional disorder), as well as to one of the *o*-chlorophenol guests in **7**, located on and orientationally disordered about the inversion centers. These disordered guests were assigned isotropic temperature factors, and were refined with a constrained geometry, in order to avoid unreliable distortions of the covalent parameters.

Lists of fractional coordinates and thermal parameters of the nonhydrogen atoms, atomic coordinates of the hydrogen atoms, as well as of bond lengths and bond angles, along with the atom labeling schemes used, have been deposited as supplementary material.

3. Results and Discussion

3.1. Coordination Polymers of Zn–TPyP

This study relates to three different types of the tetrapyridylporphyrin compounds: the zinc complex of TPyP, co-crystals of this complex with solvent guest molecules, and co-crystals of the non-metallated TPyP with solvent guest compounds. The Zn(II) complex of TPyP contains six potential ligating sites available for association with other species. The 4-coordinate zinc, located in the center of the porphyrin core, can bind additional ligands on both sides of the molecular framework, assuming either a 5-coordinate or a 6-coordinate structure. The four 4-pyridyl substituents, acting as Lewis bases, can also bind to other species (Lewis acids) through the lone-pair electrons of the peripheral nitrogen atoms.

In non-protic solvents of low polarity, a self-assembling process is expected to take place due to the favorable free-energy of binding between the pyridyl moiety and the zinc porphyrin system [1]. Indeed, crystallization of Zn–TPyP from anisole led to the formation of solvent-free, densely packed crystals. The observed

crystal structure of compound **1** is shown in Figure 2. It consists of zigzag shaped polymeric aggregates which are held together by a strong coordination between the metal center of one Zn–TPyP molecule and one of the pyridyl rings of a neighboring metalloporphyrin entity. The bridging zinc–N(porphyrin) intermolecular bond distance is 2.132 Å. The four intramolecular Zn–N(pyrrole) bond lengths are not much shorter, all being within the range of 2.054–2.098 Å. Formation of the polymeric arrangement utilises only two out of the six possible binding sites of each Zn–TPyP entity. It appears that steric constraints associated with the bulky and rigid molecular shape, and the very effective side-packing of the zigzag polymers aligned next to each other, prevent the formation of a more extensive linkage. In the 5-coordinate square-pyramidal environment of the surrounding N-ligands the metal center deviates significantly (0.31 Å), as expected, from the mean plane of the pyrrole N-atoms. This allows a relatively close approach between the concave ('back') sides of TPyP molecules from neighboring polymers related by inversion, without a significant electrostatic repulsion between the metal centers of the partly overlapping porphyrin cores (Figure 2). The relative disposition of adjacent porphyrin planes along the polymeric chain deviates slightly from perpendicularity, as has typically been observed in related structures [13].

Crystallization of Zn–TPyP from protic aromatic solvents, such as aniline, yields similarly structured polymeric patterns of the metalloporphyrin moieties. In this case, however, Zn–TPyP crystallizes as a 1 : 1 complex with aniline (**2**), the presence of the latter modifying to some extent the inter-chain organization. Figure 3 illustrates the 'herringbone' type arrangement observed in this structure. In the C-centered lattice, the two different zones of the 'herringbone' contain inversion-related layers of coplanar porphyrin molecules. As in the previous example, the zinc atom is linked to the four N-atoms of the porphyrin core at 2.060–2.081 Å, as well as to a pyridine nitrogen of an adjacent porphyrin molecule at 2.147 Å. It is also displaced by 0.32 Å from its porphyrin plane towards the coordinated pyridine ligand. The periodic translations of this packing along the *b*-axis about which the 'herringbone' pattern is formed, and thus the inclination of consequent porphyrin planes in a chain with respect to that axis, are similar in the two structures; $b = 13.825$ Å in **1** and 13.810 Å in **2**. In every porphyrin molecule the pyridyl substituent located *trans* to the zinc-coordinated one is further solvated by the aniline guest component *via* an $NH_2 \cdots$N(pyridyl) hydrogen-bonding interaction (at 2.97 Å). Accommodation of the aniline solvent, which is driven by its energetically favorable H-bond association with the porphyrin periphery [20], makes the side packing of the polymeric chains less efficient. This is reflected in an apparent orientational disorder of the non-coordinated pyridyl substituents (see above), and a slightly lower packing density.

Since the formation of the one-dimensional coordination polymers of Zn–TPyP involves ligation of only one pyridyl substituent of the TPyP molecule to the metal center of another metalloporphyrin framework, the zigzag chain structure observed in compounds **1** and **2** is quite similar to that previously reported for

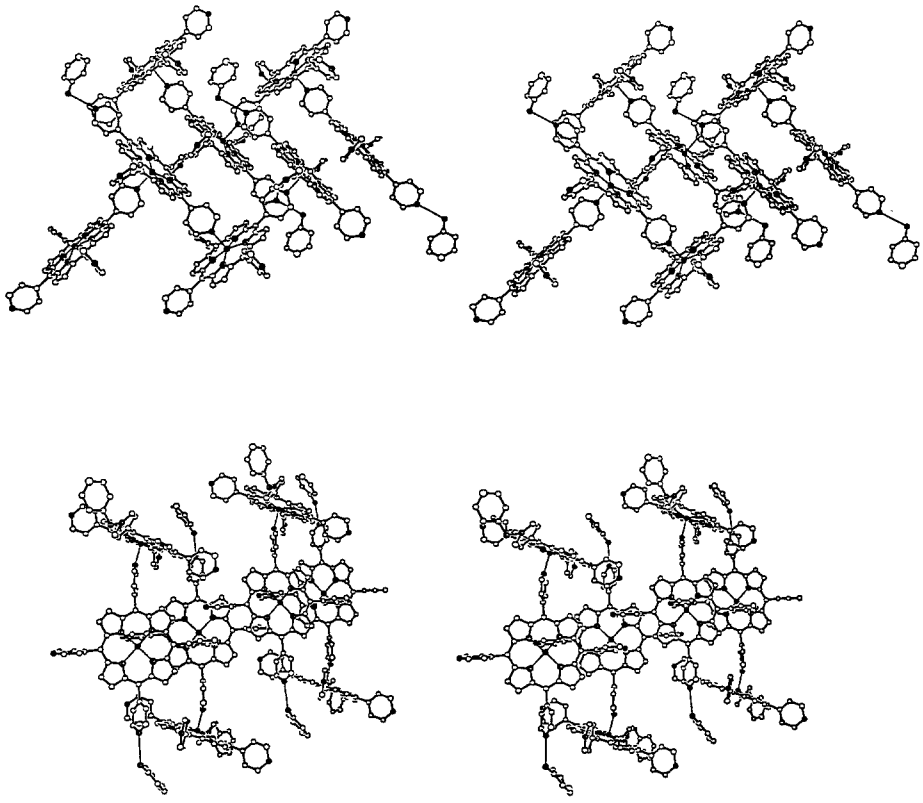

Fig. 3. Stereoviews of the coordination polymers in **2**. Two inversion-related parallel zigzag chains are shown in the upper part. The side-packing and steric fit of translation-related pairs of the polymeric chains are displayed in the lower part. All Zn–N coordinative bonds, and $NH_2\cdots N$ hydrogen bonds (involving the aniline solvate) are indicated by thin solid lines.

a monopyridyl-triphenyl-Zn-porphyrin derivative [13]. In fact, the coordination geometry around the metal center is nearly the same in all three structures (Table II), including the markedly tilted orientation of the pyridine residue with respect to the metalloporphyrin core to which it binds (Figures 2 and 3). Two additional points are of considerable significance in this context. It has already been confirmed by NMR studies that self-assembling of the polymeric aggregates, through the Zn-to-pyridyl intermolecular ligation, takes place in the solution (chloroform) as well as in the solid state [13]. Furthermore, metal centers other than zinc (e.g., Fe) can also be used as a template for the coordination-driven polymerization. The latter has been illustrated by the crystallographic investigation of tetra(*o*-nicotinamidophenyl)-Fe-porphyrin, in the structure of which a polymeric linkage is formed by the coordination of the nicotine nitrogen of one porphyrin to the Fe center of an adjacent porphyrin [14].

TABLE II. Selected structural parameters for the metalloporphyrin compounds

1	2	3	4	Zn–MPyTPP[a]
(a) *Zn–N(pyrrole) bond length range* (Å).				
2.054–2.098(9)	2.060–2.081(5)	2.052–2.074(9)	2.061–2.078(3)	2.053–2.070(6)
(b) *Zn–N(pyridine) bond length* (Å).				
2.132(9)	2.147(4)	2.364(9)	2.388(4)	2.234(7)
(c) *N(pyrrole)–Zn–N(pyridine) bond angles* (deg).				
97.0(4)	94.0(2)	83.5(3)	84.0(3)	88.1(2)
98.0(4)	96.2(2)	87.7(4)	87.2(2)	96.0(3)
98.8(4)	101.0(2)	92.3(4)	92.8(2)	99.6(2)
100.4(4)	104.9(2)	96.5(5)	96.0(3)	107.8(2)
(d) *Zn deviation from the porphyrin plane* (Å).				
0.308(3)	0.326(2)	0	0	0.285

[a] Ref. [13]

In an effort to exploit better the coordination capacity of the Zn-TPyP moiety, extensive crystallization experiments were carried out also in small polar solvents. The solvents used consisted of various mixtures of wet methanol, DMSO, acetic acid, ethyl acetate, as well as water, and were characterized by varying degrees of polarity, volatility, and capability to dissolve the tetrapyridylporphyrin derivative. These efforts have yielded, indeed, an entirely new series of solid materials, revealing novel types of coordination polymers constructed from the Zn-TPyP building blocks. Single crystals suitable for a detailed crystal structure analysis were obtained for compounds **3** and **4** from wet methanol and DMSO solutions, respectively. The two corresponding structures were found to be isomorphous (Table I), and appeared to differ only slightly in the contents of the incorporated solvent. They represent also two independent determinations at the different laboratories of the authors.

The observed interporphyrin polymeric architecture, characterized in this structure type by a trigonal symmetry, is also propagated by metal–ligand interactions. The zinc atom at the center of TPyP is located on a crystallographic inversion, and is 6-coordinate to four pyrrole nitrogens of the porphyrin core and to two pyridyl N-atoms of other porphyrins acting as axial ligands. Every porphyrin monomer is thus strongly linked to four neighboring porphyrin units. It utilizes two *trans*-related pyridyl substituents to associate with the metal center of two adjacent porphyrins along one axis, while its zinc atom binds two pyridyl functions of other monomeric units approaching from both sides of the molecular framework along a roughly perpendicular axis. The coordination distances of Zn to the core N-atoms are 2.052 and 2.074 Å in **3**, and 2.061 and 2.078 Å in **4**. In the 6-coordinate envi-

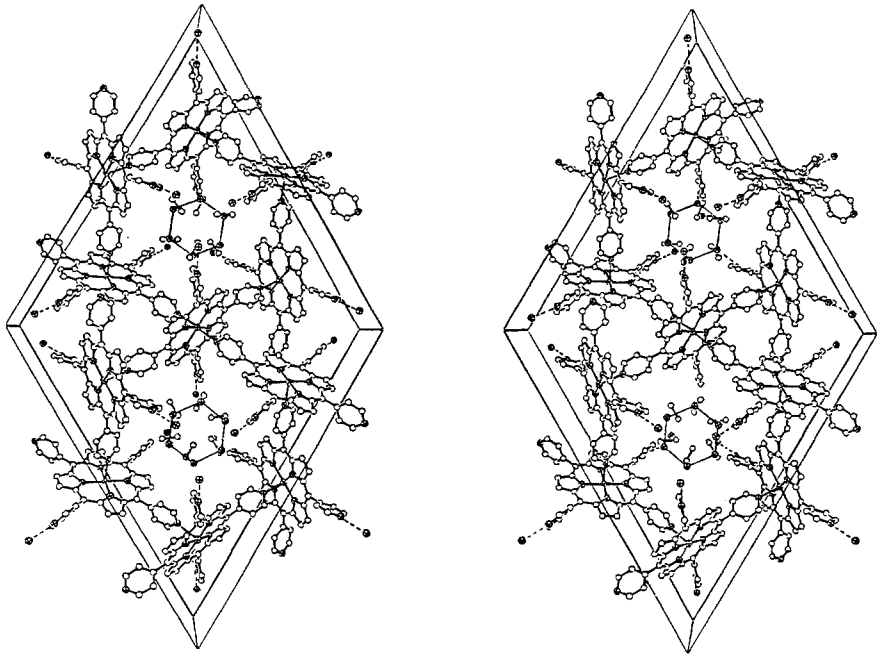

Fig. 4. Stereoview of the crystal structure of **3** down the short *c*-axis, depicting two circular polymeric patterns of Zn–TPyP. The marked hexagons represent six water molecules which are H-bonded to pyridyl groups of porphyrins located in adjacent unit-cells displaced by $\pm c$, but not included in the figure. Molecules of the methanol solvent, denoted by open circles, are displayed at the various possible sites. Alternate locations may be occupied in different cells, resulting in an overall occupancy factor of 0.5 at each site.

ronment the Zn–N(pyridyl) coordination distances, 2.364 Å in **3** and 2.388 Å in **4**, are considerably longer than those observed in the 5-coordinate moieties (see above).

The intermolecular arrangements in the crystals of **3** and **4** are illustrated in Figures 4 and 5, respectively. The structure can be described as consisting of linear polymers of Zn–TPyP molecules, which propagate in three different directions of the trigonal lattice. Extensive cross-linking of these polymers by coordination yields also six-membered circular aggregation patterns. These are centered around the threefold symmetry axes parallel to *c*, which are located between the intersection points of the linear assemblies. The other two pyridyl groups of each porphyrin are ligated by water molecules through hydrogen bonds at N···O distances of 2.83 Å in **3** and 2.85 Å in **4**. The water species provide additional bridges between the porphyrin aggregates displaced along the *c*-axis. Three molecules bound to porphyrins centered at a lower *z*-coordinate, and three other molecules linked to porphyrins centered at a higher *z*-level along *c*, form, *via* $H_2O\cdots OH_2$ hydrogen bonding, nearly planar hexagonal water clusters (See Figures 4 and 5). The cir-

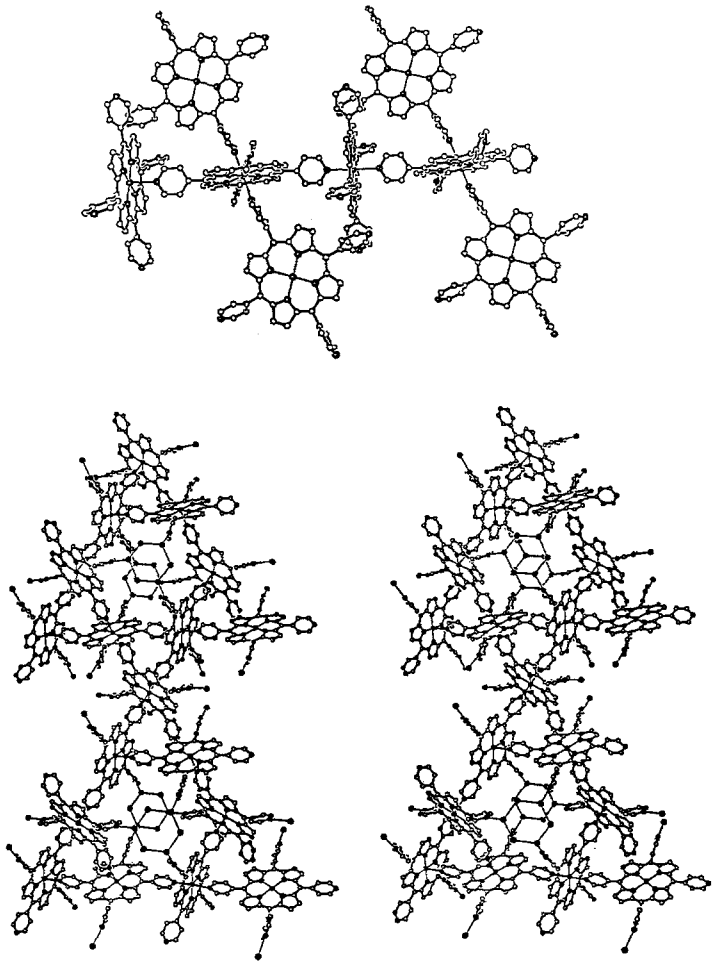

Fig. 5. Alternative illustrations of the three-dimensional polymeric structure type of Zn–TPyP, drawn using the structural parameters of compound **4**. (top) Interporphyrin fourfold coordination in directions parallel and roughly perpendicular to the porphyrin plane. (bottom) Stereoview of the interlinked linear and circular polymeric patterns of the metalloporphyrin units. Hydrogen bonding of water molecules to the pyridyl rings, and their clustering in planar hexagons which provide additional cross-linking between the polymeric aggregates, are also shown (thin solid lines). The additional water molecules trapped within the lattice between the hexagonal water clusters, but not linked directly to the pyridyl groups, are omitted for clarity.

cular polymeric porphyrin arrays interpenetrate each other in the crystal structure. Between the different $(H_2O)_6$ rings aligned perpendicularly to the *c* axis there is enough space to incorporate additional molecules of the solvent. It appears that molecules of methanol in **3**, and molecules of water in **4**, are trapped in these voids in non-stoichiometric amounts during the crystallization process (see above). The

high stability of the formed crystals, even at room temperature, suggests that the diffusion rate of the occluded molecules out of these cavities is very slow.

A somewhat related type of infinite three-dimensional polymeric network composed of Pd–TPyP building blocks has recently been described [21]. It exhibits infinite linear strips of 4-connected peripherally linked metalloporphyrin entities. The interconnection between the 4-pyridyl rings of adjacent molecules occured in that case, indirectly, through Cd(II) centers. The present study shows the first crystalline examples (**3** and **4**) of a three-dimensional coordination polymer formed by self-assembly of the tetrapyridyl-metalloporphyrin molecular frameworks through a direct interporphyrin interaction, with the porphyrin metal center acting as a templating agent.

The geometric parameters for the Zn–TPyP monomer are similar to those observed in the crystal structures of other porphyrin compounds [3], and show no unusual features. The individual pyrrole rings in **1–4** are perfectly planar, but the plane of the porphyrin core exhibits a minor ruffling [22]. The dihedral angles between the normals to these rings vary within 0.1–5.0° in **1**, 2.1–7.8° in **2**, 0.0–6.7° in **3**, 0.0–6.6° in **4**. Selected structural parameters involving the porphyrin metal center are summarized in Table II.

3.2. Aggregation and Coordination Features of TPyP

Structural investigations were also carried out on the non-metallated tetrapyridyl porphyrin in order to ellucidate the characteristic modes of interporphyrin packing and guest coordination of this compound in the solid state. Alcohols are usually very good proton donors. Therefore, further preparative efforts centered on TPyP interaction with various hydroxylic solvents. Representative examples, for which samples suitable for X-ray diffraction study could be obtained, involve co-crystals of TPyP with guaiacol (**5**), with benzyl alcohol (**6**), and with *o*-chlorophenol (**7**).

The crystal structures of compounds **5** and **6** are both centrosymmetric, with the tetrapyridylporphyrin molecules located on centers of inversion, showing similar characteristics. They consist of tightly packed layers of the porphyrin molecules, extending parallel to the *ab* plane of the unit-cell on a two-dimensional grid of 6.4–6.8 × 10.1–10.3 Å. The porphyrins are stacked in an offset manner, the mean planes of the porphyrin cores being roughly parallel to each other and roughly perpendicular to the layer (Figures 6 and 7). In this offset stacked geometry, each porphyrin core is sandwiched between two pyridyl arms of adjacent species from above and below, which are displaced by $\pm b$. Within the layer, the *trans*-related pyridyl groups of neighboring coplanar porphyrins overlap effectively, stabilizing the layered arrangement by favourable dipolar and dispersive interactions. In both structures, the pyridyl substituents directed outwards (perpendicular to the layers) are coordinated to guest/solvate molecules *via* N:···HO hydrogen bonds at 2.82 Å in **5** and 2.79 and 2.85 Å in **6**. Correspondingly, the stacking distance of the porphyrin layers in the third dimension of the crystal (along *c*) is most sensitive to

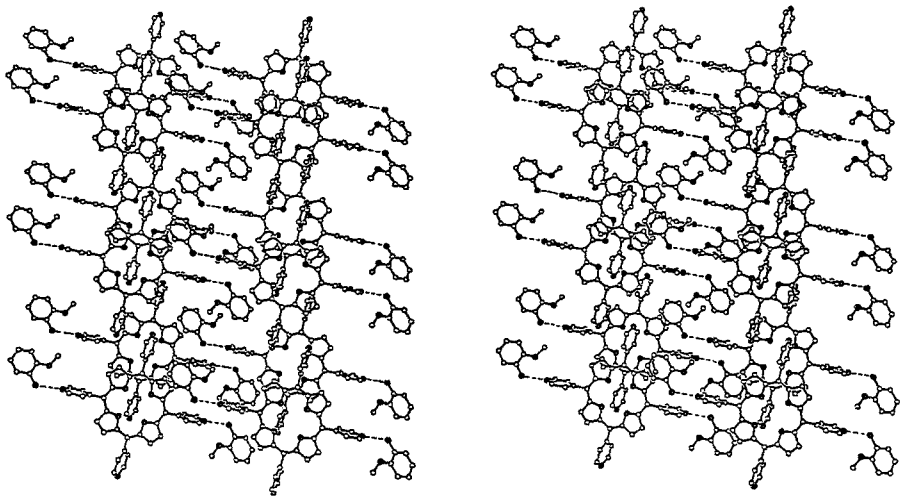

Fig. 6. The layered porphyrin arrangement and interlayer packing in **5**, illustrating the characteristic offset-stacking mode of adjacent porphyrins within the layers, and the effective coordination of the guaiacol guest solvent *via* hydrogen bonds perpendicular to the layers. The dipolarly favorable antiparallel arrangement of the uncoordinated pyridyl groups within the porphyrin zone of the structure should also be noted. Hydrogen atoms are omitted for clarity. Hydrogen bonds are marked by broken lines.

the size and shape of the pyridyl-associated guests. It thus varies in compounds **5** and **6** from 16.59 Å for the guaiacol molecule, to 17.41 Å for the benzyl alcohol ligand. Moreover, the higher conformational flexibility of the latter and the less dense interlayer packing along *c* in **6**, allow for a disordered arrangement of this guest in the lattice (Figure 7).

An interesting modification occurs when chloro-substituted guest solvent is used in the crystallization of TPyP. The increased acidity of *o*-chlorophenol makes this molecule a better proton donor than benzyl alcohol and guaiacol. Furthermore, the apparent tendency of chloroaromatic materials to optimize non-bonding Cl···Cl contacts may affect the crystalline arrangement as well. Intermolecular Cl···Cl interactions were found to play a major role in determining the supramolecular organization in the crystalline phases of tetra(4-chlorophenyl)porphyrin derivatives [8]. The effect of such interactions on packing patterns in molecular crystals is also well documented in the literature [23].

The observed intermolecular assembling of the *o*-chlorophenol adduct with TPyP (**7**) in the solid is shown in Figure 8. As a result of a complete solvation of the four pyridyl groups by *o*-chlorophenol, through N:···HO hydrogen bonds (at 2.70 and 2.71 Å), the tight layered arrangement of TPyP observed in the two previous examples is now disrupted. The porphyrin molecules (located on centers of inversion) still remain stacked in columns parallel to one another, with a similar offset geometry and periodic translation of 6.325 Å as in structures **5** and **6**. These

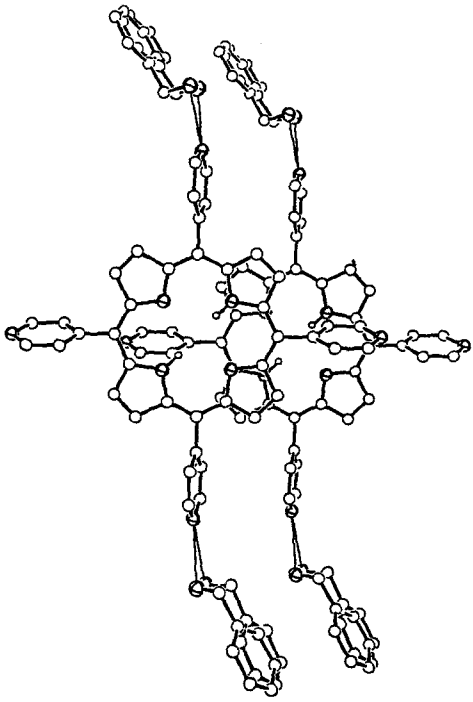

Fig. 7. Illustration of the porphyrin stacking and the disorder of the hydrogen-bonded benzyl alcohol guest in **6**. Other features of the intermolecular packing are similar to those found in **5** (see Figure 6).

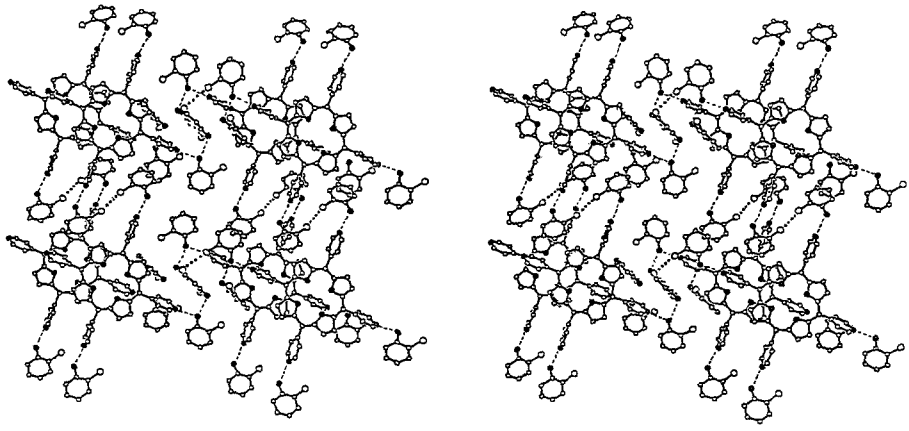

Fig. 8. Stereoview of the crystal packing in **7**, showing the columnar arrangement of the porphyrin molecules. The intricate pattern of interactions between these columns through the *o*-chlorophenol solvent guest species are also shown. Hydrogen atoms are omitted for clarity. Hydrogen bonds and Cl···Cl short contacts are denoted by dashed lines (between crossed circles) and dotted lines (between open circles), respectively.

TABLE III. Hydrogen bonds in compounds **2–7**

Compound	solvent	distance (Å)	
(a) *Porphyrin–guest/solvate interactions:*			
2	aniline	N...HN	2.97(2)
3	water	N...HO	2.83(1)
4	water	N...HO	2.85(1)
5	guaiacol	N...HO	2.817(5)
6	benzyl alcohol	N...HO	2.79(1), 2.85(1)
7	*o*-chlorophenol	N...HO	2.70(2), 2.71(2)
(b) *Solvent–solvent interactions:*			
3	water	O...HO	2.82(2)
4	water	O...HO	2.82(1)
7	*o*-chlorophenol	O...HO	2.68(4)

columns are now held together, indirectly, through the surrounding solvation shell by a complex and extensive pattern of specific intermolecular interactions. In one direction they are joined through two *o*-chlorophenol molecules, while in the other direction a chain of four guest species links adjacent columns. In the former case, involving [–TPyP–guest–guest–TPyP–] arrays, the two guests associate with one another *via* Cl···Cl contacts at 3.35 Å across the crystallographic inversion. The latter cluster, involving [–TPyP–$(guest)_4$–TPyP–] arrays, incorporates between the pyridyl-coordinated species two other *o*-chlorophenol molecules located on (and twofold disordered about) centers of inversion. It exhibits guest···guest contacts of OH···OH 2.68 Å and Cl···Cl 3.57 Å. This aggregate structure of the TPyP co-crystals with *o*-chlorophenol is thus optimally stabilized by an intricate three-dimensional pattern of hydrogen bonds and attractive halogen–halogen interactions with the participation of all polar functions of the constituent molecules. The observed 3.35 Å value for the non-bonding Cl···Cl contact is much shorter than the sum of the van der Waals radii, and lies within the lower range of previously reported data for related chloro-substituted aromatic compounds [23].

Detailed parameters of the molecular structure of TPyP are included in the supplementary material, showing no unusual features. Only a minor ruffling of the porphyrin core has been observed in structures **5–7**, the largest deviations of the individual atoms from the mean porphyrin plane not exceeding 0.14 Å. The hydrogen bonding distances between the various guest solvents and the pyridyl N-sites in structures **2–7** are summarized in Table III.

4. Conclusions

It has previously been shown that intermolecular aggregation of the bulky and partly rigid framework of tetraphenylporphyrin (both in its basic and metallat-

ed forms) is dominated by molecular shape, revealing a strong conservation of the porphyrin lattice structure [4–6]. We have also demonstrated in a more recent study [8,9], as well as in the present investigation, that it is possible to fine-tune the interporphyrin aggregation by introducing polar sensor groups into the molecular framework in order to induce specific modes of supramolecular organization. Tetrapyridylporphyrin is very similar in its overall size and shape to tetraphenylporphyrin. Yet, effective formation of one-dimensional and three-dimensional coordination polymers based on metallated TPyP, and directed by metal-to-ligand interactions, has been demonstrated in this study. This adds to our previous syntheses and characterizations of hydrogen-bonding polymers constructed from tetra(hydroxyphenyl)porphyrin and tetra(carboxyphenyl)porphyrin derivatives [8,9]. The studies on the non-metallated TPyP demonstrate that intermolecular aggregation in the solid state of polarized tetraphenylporphyrin derivatives is strongly affected by specific coordinative interactions with the crystallization (guest) solvent. These observations can be useful in empirical evaluations of the interplay of weak intermolecular forces in the porphyrin aggregates. The results shown above may indicate, for example, that in the layered arrangement of the TPyP molecules (which is also characteristic of many tetraphenylporphyrin structures [4–6]) the contribution of the offset stacking interaction to the lattice stability is more important than that of the dipolar attractions between antiparallel pyridyl rings along the other dimension of the porphyrin layer. Moreover, conservation of the interporphyrin offset stacking geometry in structures **5–7** is in agreement with previous findings that the offset geometry is a fundamental property of the porphyrin–porphyrin interaction [24]; the current results provide an empirical evidence of the particular aggregation mode preferred by the TPyP molecules (see Figure 7). Theoretical evaluations are needed to assess the relative contribution of π–π interactions and van der Waals forces to the observed stacking interaction [25]. The range of molecular recognition features referred to in this study, can readily be utilized in the design of additional new solid porphyrin materials with a desired composition and intermolecular architecture. Further structural investigations of solids based on differently functionalized tetraphenylporphyrin building blocks are currently in progress.

Acknowledgement

This research was supported in part by grant No. 90–00061 from the United States–Israel Binational Science Foundation (BSF), Jerusalem, Israel.

References

1. S. Anderson, H.L. Anderson, and J.K.M. Sanders: *Acc. Chem. Res.* **26**, 469 (1993), and references therein; I.P. Danks, I.O. Sutherland, and C.H. Yap: *J. Chem. Soc. Perkin Trans. 1* 421 (1990).
2. G.A. Schick, I.C. Schreiman, R.W. Wagner, J.S. Lindsey, and D.F. Bocian: *J. Am. Chem. Soc.* **111**, 1344 (1989).
3. W.R. Scheidt and Y.J. Lee: *Struct. Bond. (Berlin)* **64**, 1 (1987).

4. M.P. Byrn, C.J. Curtis, S.I. Khan, P.A. Sawin, R. Tsurumi, and C.E. Strouse: *J. Am. Chem. Soc.* **112**, 1865 (1990).
5. M.P. Byrn, C.J. Curtis, I. Goldberg, Y. Hsiou, S.I. Khan, P.A. Sawin, S.K. Tendick, and C.E. Strouse: *J. Am. Chem. Soc.* **113**, 6549 (1991).
6. M.P. Byrn, C.J. Curtis, Y. Hsiou, S.I. Khan, P.A. Sawin, S.K. Tendick, A. Terzis, and C.E. Strouse: *J. Am. Chem. Soc.* **115**, 9480 (1993).
7. P. Tecilla, R.P. Dixon, G. Slobodkin, D.S. Alavi, D.H. Waldeck, and A.D. Hamilton: *J. Am. Chem. Soc.* **112**, 9408 (1990).
8. I. Goldberg, H. Krupitsky, Z. Stein, Y. Hsiou, and C.E. Strouse: *Supramol. Chem.*, in press (1994).
9. I. Goldberg, H. Krupitsky, and C.E. Strouse: XVI Congress of the International Union of Crystallography, Beijing, China (1993).
10. E.B. Fleischer: *Inorg. Chem.* **1**, 493 (1962).
11. A. Stone and E.B. Fleischer: *J. Am. Chem. Soc.* **90**, 2735 (1968).
12. D.M. Collins and J.L. Hoard: *J. Am. Chem. Soc.* **92**, 3761 (1970).
13. E.B. Fleischer and A.M. Shachter: *Inorg. Chem.* **30**, 3763 (1991); A.M. Shachter, E.B. Fleischer, and R.C. Haltiwanger: *J. Chem. Soc., Chem. Commun.* 960 (1988).
14. M.J. Gunter, G.M. McLaughlin, K.J. Berry, K.S. Murray, M. Irving, and P.E. Clark: *Inorg. Chem.* **23**, 283 (1984).
15. P. Main, S.J. Fiske, S.E. Hull, L. Lessinger, G. Germain, J.P. Declercq, and M.M. Woolfson: MULTAN-80, *A System of Computer Programs for the Automatic Solution of Crystal Structures from X-Ray Diffraction Data*, University of York, England (1980).
16. G.M. Sheldrick: SHELXS-86, in *Crystallographic Computing* 3, eds. G.M. Sheldrick, C. Kruger, and R. Goddard, Oxford University Press, pp. 175–189 (1985).
17. G.M. Sheldrick: SHELX-76, *A Program for Crystal Structure Determination*, University of Cambridge, England (1976).
18. G.M. Sheldrick: SHELXL-93, *Program for the Refinement of Crystal Structures from Diffraction Data*, University of Göttingen, Germany (1993).
19. A.G. Golder, K.B. Nolan, D.C. Povey, and L.R. Milgram: *Acta Crystallogr., Section C* **44**, 1916 (1988).
20. M.C. Etter: *J. Phys. Chem.* **95**, 4601 (1991).
21. B.F. Abrahams, B.F. Hoskins, and R. Robson: *J. Am. Chem. Soc.* **113**, 3606 (1991).
22. O.Q. Munro, J.C. Bradley, R.D. Hancock, H.M. Marques, F. Marsicano, and P.W. Wade: *J. Am. Chem. Soc.* **114**, 7218 (1992).
23. G.R. Desiraju: in *Organic Solid State Chemistry*, Ed. G.R. Desiraju, Elsevier (Amsterdam), Ch. 14, pp. 519–546 (1987).
24. P. Leighton, J.A. Cowan, R.J. Abraham, and J.K.M. Sanders: *J. Org. Chem.* **53**, 733 (1988).
25. C.H. Hunter and J.K.M. Sanders: *J. Am. Chem. Soc.* **112**, 5525 (1990).